On Noise in Distributed Amplifiers at Microwave Frequencies

KARL B. NICLAS, SENIOR MEMBER, IEEE, AND BRETT A. TUCKER

Abstract—**Formulas for the noise figure, and the minimum noise figure of a multi-link distributed amplifier have been developed. In addition, a relatively simple approximation formula has been devised that predicts the minimum noise figure of a practical amplifier design with good accuracy up to frequencies of 9 GHz. Finally, after the dependence of the noise characteristics on the circuit parameters is discussed, the noise figures of a 2–18-GHz three-link module are computed and compared with those measured on an actual amplifier. The measured data across the 2–18-GHz band compare favorably with the computed results. Measurements and theory agree that only small improvements in noise figure may be achieved, when noise matching the module's input impedance.**

I. Introduction

THE PRINCIPLE of distributed amplification, when applied at microwave frequencies, has yielded extremely encouraging results. Monolithic [1] as well as hybrid amplifiers [2] have exhibited respectable gain performances over the frequency band 2–20 GHz and, due to the concept of additive amplification [3], have demonstrated good power-handling capabilities. Another parameter that is of great significance to designers and users alike is the noise figure. Hence, the dependence of the noise figure on the circuit elements has become of major interest in the design of distributed amplifiers.

Little has been reported on the noise characteristics of distributed amplifiers. In their pioneering paper on distributed amplification, E. L. Ginzton *et al.* addressed the noise behavior for the case of gridded electron tubes [3]. By adding the noise powers generated in the active devices and the grid-line terminations, the authors developed an expression for the noise figure that is based primarily on a qualitative evaluation of the amplifier's noise sources. Recently, Y. Ayasli *et al.* published the computed noise performance of a 2–12-GHz amplifier. However, except for the schematic containing the relevant noise sources, the authors did not give any details of the theory their computer program is based on [4].

It is the purpose of this paper to provide some understanding of the noise phenomenon in distributed amplifiers and to quantitatively examine the factors that determine its magnitude. Based on a rigorous analysis, it is demonstrated that the difference between the noise figure and the optimum noise figure is rather small when designing for a flat gain response across a multi-octave band. This fact was first discovered in experiments which proved it to be virtually impossible to improve the noise figure of a three-link amplifier module by means of outside tuning.

Manuscript received January 25, 1983; revised March 17, 1983.
The authors are with the Watkins-Johnson Company, Palo Alto, CA.

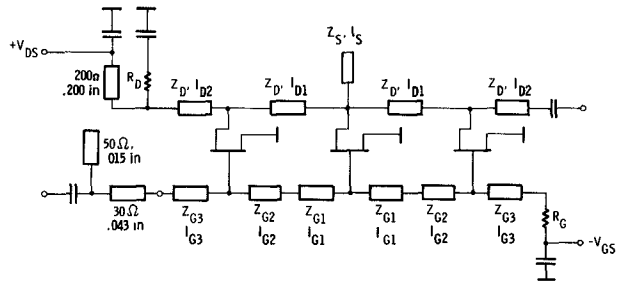

Fig. 1. Schematic of a three-link distributed amplifier.

II. Noise Parameters and Noise Figure

A. Elementary Amplifier

The formulas derived in this paper contain the noise generated by the active devices and the thermal noise agitation injected by the terminations of both idle ports. The part that may be contributed by lossy transmission line elements or lossy inductors, as well as capacitors, is considered to be comparatively small and has therefore been neglected.

The circuit diagram of a practical three-link distributed amplifier is shown in Fig. 1 [2]. The linking components between the transistors of this particular network are composed of transmission line elements of equal electrical lengths in both the gate and the drain line ($\theta_{G1} + \theta_{G2} = \theta_{D1}$). For the analysis of an amplifier such as that of Fig. 1, it is convenient to divide the module into functional blocks such as the input matching circuit, the elementary amplifiers and, if necessary, the output matching network. Hence, Fig. 2 shows the kth elementary amplifier as it will be used in the analysis of the unit's noise parameters. It incorporates the active device which is located between the gate and the drain line and described by a Π-shaped equivalent circuit. The MESFET's noise sources are characterized by the voltage v_1 and the current i_1 at the input terminal of the transistor. The input and output links of the drain and gate line may either consist of transmission line or lumped circuit elements. For reasons of simplifying the mathematical problem, it is convenient to combine both input and output links to a single input and a single output four-port and apply the concept of cascaded four-ports to the MESFET's and shunt elements as well. All circuit elements

0018-9480/83/0800-0661$01.00 ©1983 IEEE

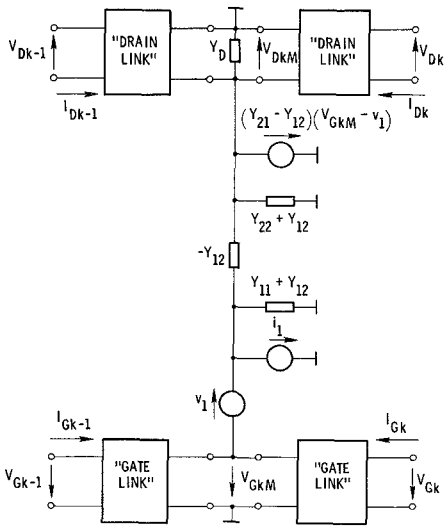

Fig. 2. Equivalent circuit of the kth elementary amplifier, including the noise sources v_1 and i_1 of the active device.

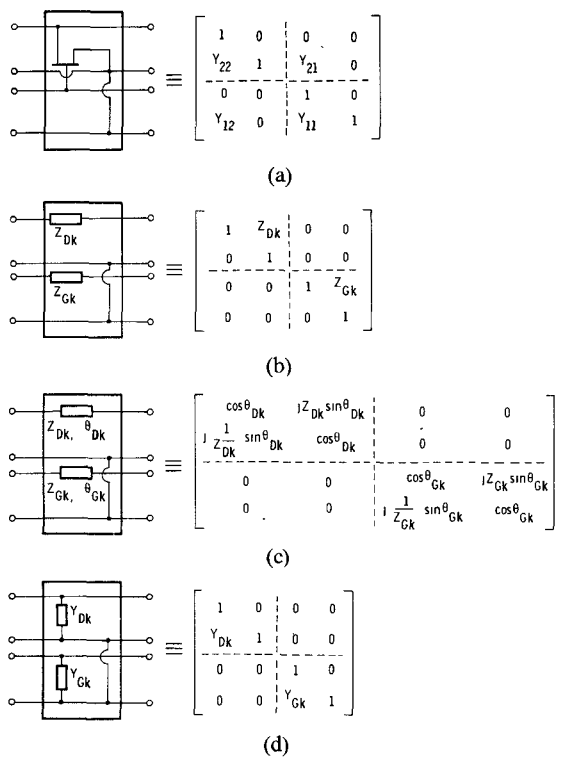

Fig. 3. Transformation matrices of the four-ports typically employed in distributed amplifier design.

as they are typically employed in a distributed amplifier can be represented by one of the four-ports shown in Fig. 3. It should be noted that the matrix for the building block of Fig. 3(d) may be used for either lumped or transmission line elements.

Now that the analytical tools have been assembled, we are able to find the voltages and currents at the drain and the gate input of the elementary amplifier of Fig. 2. They depend on the passive circuit elements, the active device and its internal noise sources (v_1 and i_1) as well as the output voltages and currents. Voltages and currents may then be expressed in form of the chain matrix equation

$$\begin{bmatrix} V_{Dk-1} \\ I_{Dk-1} \\ V_{Gk-1} \\ I_{Gk-1} \end{bmatrix} = A_k \begin{bmatrix} V_{Dk} \\ -I_{Dk} \\ V_{Gk} \\ -I_{Gk} \end{bmatrix} + B_k \begin{bmatrix} -v_{1k} \\ i_{1k} \\ 0 \\ 0 \end{bmatrix} \tag{1a}$$

where

$$A_k = A_{1k} A_{Fk} A_{2k} \tag{1b}$$

$$B_k = A_{1k} B_{Fk} \tag{1c}$$

$$B_{Fk} = \left[\begin{array}{cc:cc} 0 & 0 & 0 & 0 \\ Y_{21} & 0 & 0 & 0 \\ \hdashline 0 & 0 & 0 & 0 \\ Y_{11} & 1 & 0 & 0 \end{array}\right]. \tag{1d}$$

$[A_{1k}]$ is the matrix of the input link and $[A_{2k}]$ is that of the output link of Fig. 2, while $[A_{Fk}]$ constitutes the MESFET's chain matrix (Fig. 3(a)). All voltages and currents in (1) contain both the signal and the noise components. The matrix equation (1a) transforms the transistor's noise voltage v_1 and noise current i_1 to the input port of the elementary amplifier in Fig. 2. The transformation of $[B_{Fk}]$ depends solely on Y_{21} and Y_{11} of the active element.

Finding the relationship that exists between the input and output quantities and the internal noise sources of a multi-link module becomes now a mere exercise in matrix algebra. However, before we engage in this task, it seems appropriate to separate the signal from the noise quantities. Since we always assume to operate under linear conditions, total voltages and currents are simply the sum of their signal and noise components. The latter are symbolized by lower case letters. We therefore define for the gate side $(\ )_{Gk}$ and the drain side $(\ )_{Dk}$

$$V_{Dk,Gk} = V'_{Dk,Gk} + v_{Dk,Gk} \tag{2a}$$

$$V_{Dk-1,Gk-1} = V'_{Dk-1,Gk-1} + v_{Dk-1,Gk-1} \tag{2b}$$

$$I_{Dk,Gk} = I'_{Dk,Gk} + i_{Dk,Gk} \tag{2c}$$

$$I_{Dk-1,Gk-1} = I'_{Dk-1,Gk-1} + i_{Dk-1,Gk-1}. \tag{2d}$$

Substituting (2) into (1a) results in two matrix equations, one for the signal and one for the noise parameters. The former has been treated elsewhere [2] and is of no further concern in this paper. The noise behavior of a single link is then accurately described by

$$\begin{bmatrix} v_{Dk-1} \\ i_{Dk-1} \\ v_{Gk-1} \\ i_{Gk-1} \end{bmatrix} = A_k \begin{bmatrix} v_{Dk} \\ -i_{Dk} \\ v_{Gk} \\ -i_{Gk} \end{bmatrix} + B_k \begin{bmatrix} -v_{1k} \\ i_{1k} \\ 0 \\ 0 \end{bmatrix}. \tag{3}$$

B. Multi-Link Amplifier

1) Exact Solution: Let us now consider the amplifier's boundary conditions. The unit's idle ports are terminated with the admittances Y_{DT} on the drain and Y_{GT} on the gate side. In addition, we connect a signal source with an

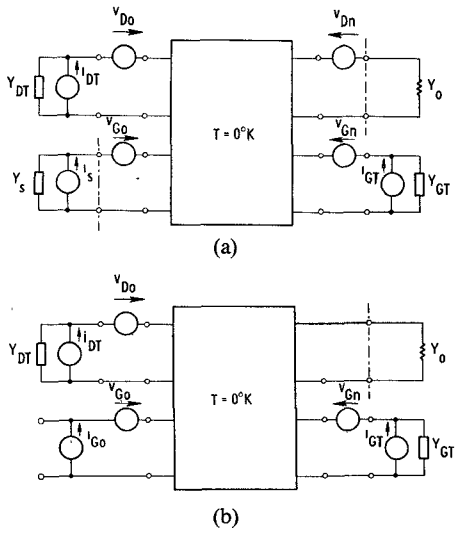

Fig. 4. Termination conditions and equivalent noise sources of the distributed amplifier for (a) the noise output power method and (b) the noise input power method.

internal admittance Y_S to the amplifier's input terminal and a load of $Y_0 = Z_0^{-1}$ to its output terminal. Since all four terminations contain a finite conductance, they inject thermal noise, which in the case of Y_S, Y_{GT}, and Y_{DT} contributes to the noise power at the amplifer's output terminal. Furthermore, those components generated by the MESFET's have a strong influence on the amplifier's noise behavior and may be represented by voltage sources at each of the four terminals. This is accomplished by transforming the transistors' individual noise sources to the four-port's terminals as illustrated in Fig. 4(a) and thereby making the four-port itself free of noise.

Applying the boundary conditions to (3) in accordance with the directions of the voltages and currents indicated in Fig. 4(a), and assuming a number of n elementary amplifiers, we derive the following matrix equation:

$$\begin{bmatrix} v_{D0} \\ -(Y_{DT}v_{D0} - i_{DT}) \\ v_{G0} \\ -(Y_s v_{G0} - i_s) \end{bmatrix} = D \begin{bmatrix} v_{Dn} \\ Y_0 v_{Dn} \\ v_{Gn} \\ (Y_{GT}v_{Gn} - i_{GT}) \end{bmatrix} + I \begin{bmatrix} v_{DF} \\ i_{DF} \\ v_{GF} \\ i_{GF} \end{bmatrix} \tag{4a}$$

where

$$D = \prod_{k=0}^{n} A_k \tag{4b}$$

$$\begin{bmatrix} v_{DF} \\ i_{DF} \\ v_{GF} \\ i_{GF} \end{bmatrix} = \sum_{k=1}^{n} \left\{ E_k \begin{bmatrix} -v_{1k} \\ i_{1k} \\ 0 \\ 0 \end{bmatrix} \right\} \tag{4c}$$

$$E_k = \left\{ \prod_{m=0}^{k-1} A_m \right\} B_k \tag{4d}$$

$$A_0 \equiv I. \tag{4e}$$

($[I]$ is the identity matrix and the links are numbered beginning at the input end.) For the simple case that all links and active devices are identical ($[A_k] = [A]$ and $[B_{Fk}] = [B]$), (4b) and (4d) take the form

$$D = A^n \tag{5a}$$

$$E_k = A^{k-1}B. \tag{5b}$$

While (4) expresses the relationship that exists between the noise parameters at the amplifier's input and output ports, it does not directly formulate the unknown voltages $(v_{D0}, v_{G0}, v_{Dn}, v_{Gn})$ as functions of the known quantities $(v_1, i_1, i_{GT}, i_{DT}, i_S)$. This is accomplished in (6):

$$\begin{bmatrix} v_{D0} \\ v_{G0} \\ v_{Dn} \\ v_{Gn} \end{bmatrix} = (K)_0 \begin{bmatrix} 0 \\ 0 \\ i_{GT} \\ i_{DT} \\ i_s \end{bmatrix} + \sum_{k=1}^{n} (K)_k \begin{bmatrix} v_{1k} \\ i_{1k} \\ 0 \\ 0 \\ 0 \end{bmatrix}. \tag{6}$$

(The elements of $[K]_0$ and $[K]_k$ are contained in the Appendix.)

Up to this point it was convenient to treat the problem with the technique of cascading four-ports. However, since the noise parameters responsible for the amplifier's noise figure can now be determined with (6) we abandon the four-port representation. Aside from the noise input power, the computation of the amplifier's noise figure only requires the knowledge of the noise output power. We therefore need to extract the noise voltage v_{Dn} from (6) which can be expressed by the two-port equation

$$v_{Dn} = \sum_{k=1}^{n} [(K_{31})_k v_{1k} + (K_{32})_k i_{1k}] + (K_{33})_0 i_{GT} + (K_{34})_0 i_{DT} + (K_{35})_0 i_s. \tag{7}$$

Its elements K_{ij} depend on D_{ij} and E_{ij} of (4) and the termination admittances at the amplifier's four ports. The noise power at the unit's output is in accordance with Fig. 4(a)

$$N_{Dn} = Y_0 \overline{|v_{Dn}|^2}. \tag{8}$$

In order to determine its magnitude, we now make the valid assumption that no correlation between any noise voltages or noise currents exist except for the voltage v_1 and the current i_1 of the same active device. It is usually expressed in terms of the correlation admittance Y_{cor} [5]

$$i_1 = i_n + Y_{cor} v_1 \tag{9}$$

where i_n represents that part of the current i_1 that is not correlated with v_1. By substituting (9) into (7) we are in a position to express the amplifier's noise output voltage in terms of parameters that are not correlated with each other.

$$v_{Dn} = \sum_{k=1}^{n} [(K'_{31})_k v_{1k} + (K_{32})_k i_{nk}] + (K_{33})_0 i_{GT} + (K_{34})_0 i_{DT} + (K_{35})_0 i_s \tag{10a}$$

with

$$(K'_{31})_k = (K_{31})_k + (Y_{cor})_k (K_{32})_k. \tag{10b}$$

Taking into consideration that noise correlation exists only between sources of the same active device, we obtain with (8) and (10)

$$N_{Dn} = Y_0 \left[\sum_{k=1}^{n} \left\{ |K'_{31}|_k^2 \overline{|v_1|_k^2} + |K_{32}|_k^2 \overline{|i_n|_k^2} \right\} + |K_{33}|_0^2 \overline{|i_{GT}|^2} + |K_{34}|_0^2 \overline{|i_{DT}|^2} + |K_{35}|_0^2 \overline{|i_s|^2} \right]. \tag{11}$$

Replacing the voltages and currents of (11) with the MESFETs' equivalent noise parameters as well as the noisy components of the termination admittances leads to

$$N_{Dn} = 4kT_0 \Delta f Y_0 \left[\sum_{k=1}^{n} \left\{ |K'_{31}|_k^2 R_{nk} + |K_{32}|_k^2 G_{nk} \right\} + |K_{33}|_0^2 G_{GT} + |K_{34}|_0^2 G_{DT} + |K_{35}|_0^2 G_s \right]. \tag{12}$$

With the available input noise power

$$N_S = kT_0 \Delta f \tag{13}$$

and the unit's overall gain

$$\text{Gain} = 4|K_{35}|_0^2 G_S Y_0 \tag{14}$$

we are now ready to formulate the noise figure of the multi-link distributed amplifier

$$F = 1 + \frac{1}{|K_{35}|_0^2 G_s} \times \left[\sum_{k=1}^{n} \left\{ |K'_{31}|_k^2 R_{nk} + |K_{32}|_k^2 G_{nk} \right\} + |K_{33}|_0^2 G_{GT} + |K_{34}|_0^2 G_{DT} \right]. \tag{15}$$

The computation of the minimum noise figure $F_{\min}$, the equivalent noise resistor R_n^I, the equivalent noise conductance G_n^I, and the correlation admittance $Y_{cor}^I = G_{cor}^I + jB_{cor}^I$ of the amplifier may then be accomplished by computing the noise figures (15) for four arbitrary but different input admittances Y_s and use the resulting noise figures to determine these quantities. Since the method is straightforward, it is not reported here.

While the formula (15) of the noise figure is based on the noise output power (12), it may as well be derived by transforming all noise sources in accordance with the equivalent circuit of Fig. 4(b) to the amplifier's input. Such a transformation leads to the direct formulation of the noise parameters R_n^I, G_n^I, and Y_{cor}^I which in turn can be used to calculate the noise figure F and the minimum noise figure $F_{\min}$. In pursuing this method we found the results to be in total agreement with those of the "output power method" proving its validity when applied to four-ports. Both approaches lead to identical results and neither seems to have advantages over the other regarding the computer programming.

2) Low Frequency Model: Due to the complexity of the formulas presented so far, it might be beneficial to analyze a simplified model of the multi-link amplifier. For this purpose we choose the low frequency model for which the transforming characteristics of the linking elements may be neglected. In other words, we treat the amplifier as a lossy match amplifier with n numbers of parallel transistors. The noise characteristics of this amplifier model are described by the parameters [6]

$$R_n^I = \frac{1}{n} \left[R_n + \frac{G_{DT}}{n|Y_{21}|^2} \right] \tag{16a}$$

$$G_n^I = G_{GT} + n \left[G_n + |Y_{11} - Y_{cor}|^2 \frac{G_{DT} R_n}{n|Y_{21}|^2 R_n + G_{DT}} \right] \tag{16b}$$

$$Y_{cor}^I = Y_{GT} + n \left[Y_{cor} + (Y_{11} - Y_{cor}) \frac{G_{DT}}{n|Y_{21}|^2 R_n + G_{DT}} \right]. \tag{16c}$$

If we further assume that

$$G_{DT} \ll n|Y_{21}|^2 R_n \tag{17a}$$

$$G_{DT} \ll \frac{|Y_{21}|^2}{|Y_{11} - Y_{cor}|^2} (G_{GT} + nG_n) \tag{17b}$$

$$G_{DT} \ll |Y_{21}|^2 R_n \frac{G_{GT} + nG_{cor}}{G_{11} - G_{cor}} \tag{17c}$$

which are satisfied in most practical cases the formula for the approximate minimum noise figure of a multi-link distributed amplifier takes the simple form

$$F_{\min} \cong 1 + 2 \left[R_n \left(\frac{G_{GT}}{n} + G_{cor} \right) + \sqrt{R_n \left(\frac{G_{GT}}{n} + G_n \right) + R_n^2 \left(\frac{G_{GT}}{n} + G_{cor} \right)^2} \right]. \tag{18}$$

It clearly indicates that the minimum noise figure of a distributed amplifier at low frequencies may be reduced by increasing the number of links. We will briefly investigate in Section III to what extent the approximation formula (18) may be used to determine the minimum noise figure of a multi-link distributed amplifier.

III. Computed Noise Figures and Gains of Practical Amplifier Designs

In this chapter we discuss the computed noise figure, minimum noise figure, and gain for a number of practical amplifier designs as they depend on various circuit parameters. The noise figure computations are based on (15), while the small signal gain has been computed by means of (14).

A. Cascading of Identical Links

Let us first study the case of an amplifier that consists of identical elementary blocks (Fig. 5) cascaded to a multi-link chain and terminated with R_G and R_D at the idle ports.

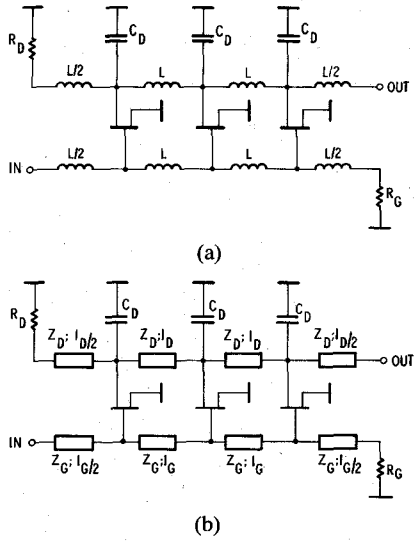

Fig. 5. Schematic of a three-link distributed amplifier with (a) lumped elements and (b) distributed line elements.

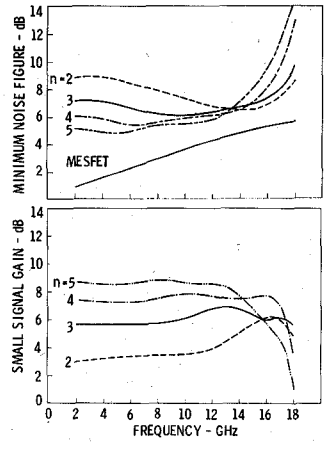

Fig. 6. Dependence of the minimum noise figure and the small signal gain of a lumped element amplifier with identical links on the number of links ($L/2 = 0.3125$ nH, $C_D = 0.159$ pF, $R_G = 38\ \Omega$, $R_D = 125\ \Omega$).

The characteristics of the MESFET used in all of the theoretical and practical studies reported here have been described in the literature [2]. The minimum noise figure and the small signal gain of a distributed amplifier employing identical links composed of lumped circuit elements in accordance with the schematic of Fig. 5(a) are shown in Fig. 6. The circuit's components $L/2$, C_D, R_G, and R_D have been optimized in order to obtain a flat gain response between 2 and 18 GHz for the case of a three-link unit. The curves of the minimum noise figure clearly demonstrate the influence of the number of elementary amplifiers at lower frequencies. However, at frequencies above 13 GHz, the minimum noise figure does not experience any improvement by cascading additional blocks. To the contrary, the parasitics of the MESFET's cause a deterioration of the overall noise performance.

Similar characteristics are exhibited in Fig. 7 when replacing the lumped elements by transmission line elements for $C_D = 0$ in accordance with Fig. 5(b). While for this case

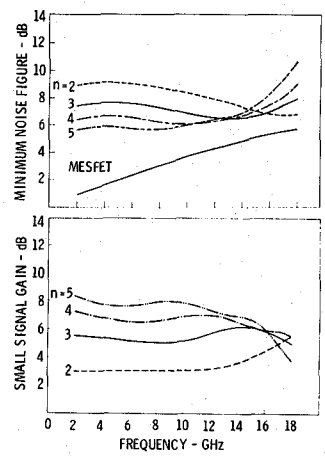

Fig. 7. Dependence of the minimum noise figure and the small-signal gain of a transmission line element amplifier with identical links on the number of links ($Z_G = Z_D = 125\ \Omega$, $l_G = 0.037$ in and $l_D = 0.057$ in, $C_D = 0$, $R_G = 38\ \Omega$, $R_D = 125\ \Omega$).

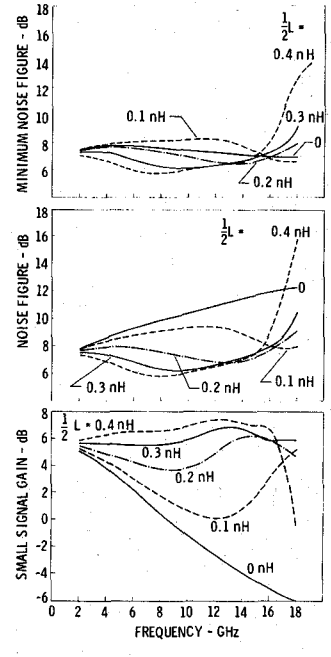

Fig. 8. Influence of the link inductance on minimum noise figure, noise figure, and small signal gain of a three-link lumped element amplifier ($C_D = 0.159$ pF, $R_G = 38\ \Omega$, $R_D = 125\ \Omega$).

the minimum noise figure shows slightly higher values at low frequencies, it is appreciably lower at the high frequency end of the band. The dependency of the noise characteristics and the small-signal gain on the inductance $L/2$ are displayed in Fig. 8 for a three-link module. The curves of the noise figure and gain include the case of our low frequency model for which we chose $L = 0$. They demonstrate that in this particular example (18) offers an acceptable approximation for the amplifier's minimum noise figure up to frequencies of 16 GHz. In addition, the plotted curves express the significance of the linking element's inductance $L/2$ on the amplifier's noise figure and its gain. Similarly, when employing transmission line elements, we find that for $n = 3$, $R_G = 38\ \Omega$, $R_D = 125\ \Omega$, $Z_G = Z_D = 125$

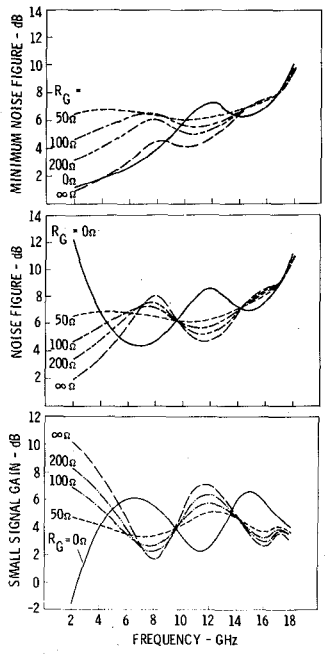

Fig. 9. Influence of the gate termination resistance on the minimum noise figure, noise figure, and small-signal gain of a three-link lumped element amplifier ($L/2 = 0.3125$ nH, $C_D = 0.159$ pF, $R_D = 125\ \Omega$).

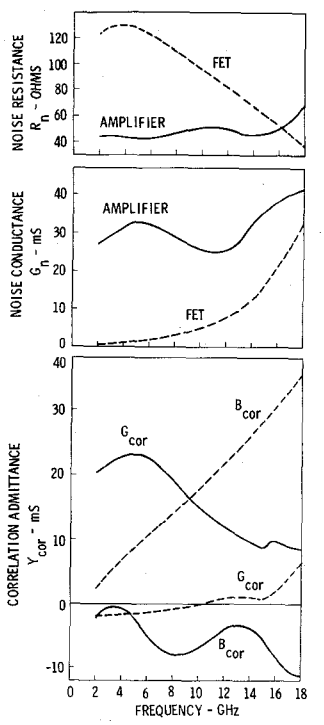

Fig. 10. The equivalent noise parameters of the three-link equal line lengths amplifier of Fig. 1 and Table I (solid curves) and the MESFET (dashed curves).

Ω, $l_G = 0.037$ in, and $l_D = 0.057$ in, the minimum noise figure computed with (15) deviates from its approximation (18) by only ± 0.85 dB between 2 and 18 GHz.

Let us now investigate the dependence of the amplifier's performance parameters on the magnitude of the resistors terminating the idle ports. The influence of the gate resistance on minimum noise figure, noise figure, and small-signal gain is plotted in Fig. 9 for a three-link module ($\frac{1}{2}L = 0.3125$ nH, $C_D = 0.159$ pF, and $R_D = 125\ \Omega$). The curves demonstrate that the magnitude of R_G has its greatest impact on all three parameters at the low frequency end of the band. Since R_G determines to a great extent the magnitude of the gain variation across the band, the requirement of a flat gain response over a very wide band leaves little freedom to improve the noise figure by means of R_G. As expected, the amplifier's noise figures experience little change with the terminating resistance R_D. Both, minimum noise figure and noise figure do not differ by more than 1.7 dB for $0 \leqslant R_D \leqslant \infty$ over the 2–18-GHz band. However, the right choice of R_D is important for a flat gain performance at lower frequencies. The performance characteristics of the distributed amplifier employing high impedance transmission line elements and their dependence on the individual circuit parameters are essentially very similar to those incorporating lumped elements.

B. The Equal Line Lengths Amplifier

In this section we examine the noise characteristics of an amplifier that employs transmission lines of equal lengths between the active elements [2]. This approach has the advantage of placing MESFET's between two parallel straight lines resulting in a very simple structure. The schematic of a three-link module designed for the 2–18-GHz frequency band is shown in Fig. 1. The magnitudes of its elements are listed in Table I while a detailed description of the unit's fabrication can be found elsewhere [2]. The amplifier's computed, noise parameters R_n, G_n, and Y_{cor} are plotted in Fig. 10 which also contains the noise parameters of the MESFET. As expected, at low frequencies, we are essentially paralleling the noise resistances R_n of the three transistors, while the noise conductance G_n is mainly dependent on the resistance R_G of the gate line's termination. Similarly, G_{cor} depends almost entirely on R_G at low frequencies. It is also apparent from these curves that the noise parameters of the amplifier are confined to a much narrower range than those of the transistor, suggesting much less variation of the amplifier's minimum noise figure versus frequency. This is easily discernable when comparing the optimum noise figures of the three-link

TABLE I
ELEMENT VALUES OF THE THREE-LINK MODULE WITH EQUAL LINE LENGTHS

$Z_{G1} = 65\Omega$	$\Theta_{G1} = 12.2°$	$l_{G1} = .020$ in
$Z_{G2} = 87\Omega$	$\Theta_{G2} = 20.7°$	$l_{G2} = .034$ in
$Z_{G3} = 87\Omega$	$\Theta_{G3} = 15.2°$	$l_{G3} = .025$ in
$Z_{D1} = 140\Omega$	$\Theta_{D1} = 32.9°$	$l_{D1} = .054$ in
$Z_{D2} = 140\Omega$	$\Theta_{D2} = 6.7°$	$l_{D2} = .011$ in

$R_G = 38\Omega$
$R_D = 125\Omega$

(DEGREES AT 20 GHz)

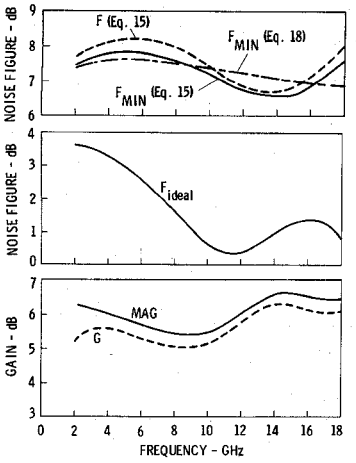

Fig. 11. Noise figures and small signal gains of the three-link equal line lengths amplifier (Fig. 1 and Table I).

device (Fig. 11) with those of the MESFET (Fig. 6). As evidenced by the curves in Fig. 11, there is little difference between the minimum noise figure and the noise figure as computed for a 50-Ω system. The same is true for the maximum available gain and the insertion gain measured when operating between a 50-Ω source and a 50-Ω load. The former can be easily verified in an experiment designed to improve the unit's noise figure by means of noise matching. As a matter of fact, it was the result of such an experiment that aroused our curiosity and prompted the investigation reported in this paper. For the designer, it is of interest to know the extent to which the terminations of the idle ports are contributing to the overall noise figure. For this reason we have computed the noise figure of the amplifer incorporating ideal MESFET's, i.e., for devices that are totally noiseless. As demonstrated by F_{ideal} in Fig. 11, the influence of mainly R_G on the amplifier's noise figure at low frequencies is significant. The curve explains why the unit's noise figure at low frequencies is so much higher than that of the individual transistor. Finally, a comparison of the optimum noise figures as computed with the exact formula (15) and the approximation formula (18) demonstrates the validity of (18) at frequencies up to 9 GHz for this design (Fig. 11).

IV. Experimental Verification

In order to support the theoretical results, a three-link amplifier module was constructed and its noise figure measured. The topology of this unit is identical to that of Fig. 1 with the element values listed in Table I. Its fabrication is described in a previous paper [2] which also discusses the module's small-signal gain, reflection loss, and reverse isolation characteristics. The noise parameters of the MESFET are plotted in Fig. 10 as dashed curves. They are derived from measurements performed on a single transistor biased at a drain voltage and a drain current ($V_{ds} = 4$ V, $I_{ds} = 42$ mA) representative for the MESFET's operation in the amplifier. While painstaking efforts were taken to measure the data leading to the computation of the MESFET's noise parameters, the accuracy of the results was only fair and was especially compromised in the area of correcting the noise figure for the tuner losses. Considering these errors and taking into account the performance tolerances of the devices, the agreement between theoretically predicted (15) and measured noise figures is surprisingly close as evidenced by the comparison of Fig. 12. It is interesting to note how well the approximation formula of the minimum noise figure (18) predicts the actual computed and measured noise figures. The reason is based on two observed facts. First, there is little difference between the minimum and the actual noise figure in a distributed amplifier. Second, the transformation properties of its linking elements seem to have nearly the same effect on the amplifier's noise figure as noise matching has on the noise figure of the equivalent lossy-match amplifier.

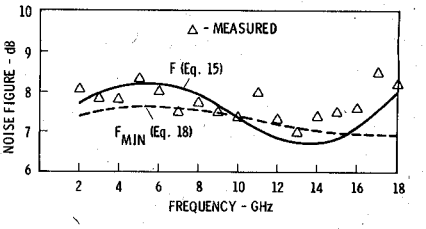

Fig. 12. Comparison of the exact (15), the approximated (18), and the measured noise figures of the three-link equal line lengths amplifier.

V. Conclusion

A set of formulas has been developed that makes it possible to compute the noise parameters and noise figures of distributed amplifier modules consisting of n arbitrary links. Based on these theoretical expressions, the noise figures' dependence on the circuit parameters was studied. As a result, it was found that improving the noise figure by altering individual circuit parameters compromises the gain performance of the amplifier whenever ultra-broad-band performance is desired. Due to the complexity of the accurate formulas, an attempt was made to generate approximation formulas designed to replace the accurate noise figure expressions under low frequency conditions. These formulas predict the noise figure of a practical amplifier design up to 9 GHz with good accuracy and, most important, contribute to the understanding of the noise phenomenon at lower frequencies.

Even though the accuracy in our measurements of the device's optimum noise figure leading to the equivalent noise parameters is fair, the agreement between measured and computed data was very encouraging. Finally, our initial measurements indicating little difference between the noise figure and the minimum noise figure of a practical three-link amplifier design were theoretically supported by the computed results.

Appendix
The Elements of $[K]$

The noise voltages at the four terminals of the multi-link amplifier are expressed by (6) as functions of the active devices' noise parameters v_1 and i_1, the noise currents generated by the idle ports' terminations i_{GT} and i_{DT}, as

well as the noise current of the source impedance i_s. The output noise voltage v_{Dn} is formulated in (7) and its elements are

$$(K_{31})_k = \frac{1}{C}\{C_1[(E_{21})_k + Y_{DT}(E_{11})_k] - C_2[(E_{41})_k + Y_s(E_{31})_k]\} \quad \text{(A1a)}$$

$$(K_{32})_k = -\frac{1}{C}\{C_1[(E_{22})_k + Y_{DT}(E_{12})_k] - C_2[(E_{42})_k + Y_s(E_{32})_k]\} \quad \text{(A1b)}$$

$$(K_{33})_0 = \frac{1}{C}\{C_1[D_{24} + Y_{DT}D_{14}] - C_2[D_{44} + Y_sD_{34}]\} \quad \text{(A1c)}$$

$$(K_{34})_0 = \frac{C_1}{C} \quad \text{(A1d)}$$

$$(K_{35})_0 = -\frac{C_2}{C} \quad \text{(A1e)}$$

$$C_1 = D_{43} + Y_{GT}D_{44} + Y_s(D_{33} + Y_{GT}D_{34}) \quad \text{(A1f)}$$

$$C_2 = D_{23} + Y_{GT}D_{24} + Y_{DT}(D_{13} + Y_{GT}D_{14}) \quad \text{(A1g)}$$

$$C = C_1[D_{21} + Y_0D_{22} + Y_{DT}(D_{11} + Y_0D_{12})] - C_2[D_{41} + Y_0D_{42} + Y_s(D_{31} + Y_0D_{32})]. \quad \text{(A1h)}$$

ACKNOWLEDGMENT

The authors wish to thank R. R. Pereira, who performed the measurements and the tuning of the amplifiers. Thanks go also to W. T. Wilser in whose Department the GaAs MESFET's were fabricated. The authors are indebted to R. Mendiola who typed the complicated formulas.

REFERENCES

[1] Y. A. Ayasli, L. D. Reynolds, J. L. Vorhaus, and L. Hanes, "Monolithic 2–20 GHz GaAs traveling-wave amplifier," *Electron. Lett.*, vol. 18, pp. 596–598, July 1982.

[2] K. B. Niclas, W. T. Wilser, T. R. Kritzer, and R. R. Pereira, "On theory and performance of solid-state microwave distributed amplifiers," *IEEE Trans. Microwave Theory Tech.*, vol. MTT-31, June 1983.

[3] E. L. Ginzton, W. R. Hewlett, J. H. Jasberg, and J. D. Noe, "Distributed amplification," *Proc. IRE* vol. 36, pp. 956–969, Aug. 1948.

[4] Y. A. Ayasli, R. L. Mozzi, J. L. Vorhaus, L. D. Reynolds, and R. A. Pucel, "A monolithic GaAs 1–13 GHz traveling-wave amplifier," *Trans. Microwave Theory Tech.*, vol. MTT-30, pp. 976–981, July 1982.

[5] H. Rothe and W. Dahlke, "Theory of noisy four-poles," *Proc. IRE*, vol. 44, pp. 811–818, June 1956.

[6] Karl B. Niclas, "The exact noise figure of amplifiers with parallel feedback and lossy matching circuits," *Trans. Microwave Theory Tech.*, vol. MTT-30, pp. 832–835, May 1982.

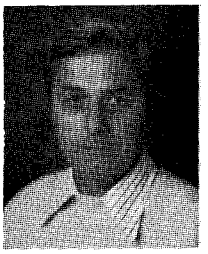

Karl B. Niclas (M'63–SM'81) received the Dipl.—Ing. and Doctor of Engineering degrees from the Technical University of Aachen, Aachen, Germany, in 1956 and 1962, respectively.

From 1956 to 1962 he was with the Microwave Tube Laboratory at the Telefunken G.m.b.H. Tube Division, Ulm-Donau, Germany. He was engaged in research and development on ultra-low-noise and medium-power traveling-wave tubes. In 1958 he became Head of the company's Traveling-Wave Tube Section and Assistant Manager of the Microwave Tube Laboratory. From 1962 to 1963 he was associated as a Senior Project Engineer with General Electric Microwave Laboratory, Stanford, CA. His work was mainly concerned with theoretical and experimental investigations of single-reversal focused low-noise traveling-wave tube amplifiers, and resulted in the first lightweight amplifier of this type. In 1963 he joined the Technical Staff of Watkins–Johnson Company, Palo Alto, CA, and is presently Consultant to the Vice President, Devices Group. His current research efforts are primarily focused on advanced GaAs FET amplifiers, broad-band power combining techniques, and wide-band GaAs FET oscillator concepts. From 1967 to 1976 he was Manager of the company's Tube Division. Before that, he was Head of the Low-Noise Tube R & D Section, and prior to that he was engaged in a research program on new concepts for achieving high efficiency in traveling-wave tubes. He is the author of numerous papers and holds a number of patents.

Dr. Niclas received the outstanding publications award in 1962 of the German Society of Radio Engineers.

Brett A. Tucker was born in Elizabeth, NJ, on January 13, 1951. He received the B.S. degree in physics from the California Institute of Technology in 1973.

In 1980 he joined Watkins–Johnson Company, Palo Alto, CA, where he has been working on the design of monolithic GaAs MIC's as well as broad-band hybrid amplifiers. He is also currently a Ph.D. candidate at the University of California at Berkeley, where his area of research is microwave applications of Josephson junctions.

Mr. Tucker is a member of Tau Beta Pi.